



**HAL**  
open science

## Synthesis and characterization of polystyrene-*b*-poly(vinyldipicolinic acid) pH-responsive core-shell nanoparticles

Abdel Wahab Mouhamad, Tamara Elzein, Nadine Barroca-Aubry, Eric Simoni, Nael Berri, François Brisset, Vincent Huc, Philippe Roger

► **To cite this version:**

Abdel Wahab Mouhamad, Tamara Elzein, Nadine Barroca-Aubry, Eric Simoni, Nael Berri, et al.. Synthesis and characterization of polystyrene-*b*-poly(vinyldipicolinic acid) pH-responsive core-shell nanoparticles. *European Polymer Journal*, 2023, 201, 10.1016/j.eurpolymj.2023.112541 . hal-04305125

**HAL Id: hal-04305125**

**<https://hal.science/hal-04305125v1>**

Submitted on 27 Nov 2023

**HAL** is a multi-disciplinary open access archive for the deposit and dissemination of scientific research documents, whether they are published or not. The documents may come from teaching and research institutions in France or abroad, or from public or private research centers.

L'archive ouverte pluridisciplinaire **HAL**, est destinée au dépôt et à la diffusion de documents scientifiques de niveau recherche, publiés ou non, émanant des établissements d'enseignement et de recherche français ou étrangers, des laboratoires publics ou privés.

# Synthesis and characterization of polystyrene-b-poly(vinyldipicolinic acid) pH-responsive core-shell nanoparticles.

Abdel Wahab Mouhamad<sup>a,b</sup>, Tamara Elzein<sup>a,\*</sup>, Nadine Barroca-Aubry<sup>b</sup>, Eric Simoni<sup>b</sup>, Nael Berri<sup>a,b</sup>, François Brisset<sup>b</sup>, Vincent Huc<sup>b</sup>, Philippe Roger<sup>b,\*</sup>

<sup>a</sup> Lebanese Atomic Energy Commission, National Council for Scientific Research (CNRS-L), Beirut, Lebanon

<sup>b</sup> Institut de Chimie Moléculaire et des Matériaux d'Orsay (ICMMO), Université Paris-Saclay, CNRS, 91405, Orsay, France

## 1. Abstract

In this paper, the self-assembly of a new series of amphiphilic polystyrene-b-poly(4-vinyldipicolinic acid) PS-b-PVDPA diblock copolymers in aqueous solution is reported in order to obtain core-shell nanoparticles composed of a PS core and a PVDPA shell. Diblock copolymers were synthesized by Supplemental Activation Reducing Agent-Atom Transfer Radical Polymerization (SARA-ATRP) with a degree of polymerization (DP) of the PS block in the range 113-600 and a DP of PVDPA block of 10, 30 or 50. Anionic latex nanoparticles of PS-b-PVDPA were prepared by solvent displacement methods. All the nanoparticle suspensions had a narrow size distribution ( $0.014 \leq \text{PDI} \leq 0.144$ ) with zeta potential in the range -27 mV to -38 mV indicating strong electrostatic repulsions due to carboxylate anions and therefore high colloidal stability. DLS was used to determine nanoparticle size, with SEM and TEM used to determine and confirm both size and spherical shape. All three methods found the size for these nanoparticles to be in the range 75-120 nm. Using fluorimetry and DLS methods, Critical Micelle Concentration (CMC) for each type of nanoparticle was determined to be within the range of 33-69 mg/L, the lowest CMC was obtained for the micelle of highest PVDPA DP of 50. Micelles were pH-responsive with stability in aqueous conditions for  $\text{pH} > 3.5$ . Micelles were stable at pH 5.5 for up to 40 days and at temperature up to 60°C.

**Keywords:** Amphiphilic diblock copolymer; self-assembly; anionic nanoparticles; CMC; pH-responsive.

## 2. Introduction

Special attention has been dedicated to amphiphilic block copolymers, which undergo spontaneous self-assembly in hydrophobic or hydrophilic environments, and form supramolecular structures with a high degree of ordering of copolymer chains [1][2]. The use of block copolymer colloidal systems has been reported in a wide field of applications, such as smart gels [3] controlled drug delivery systems [4][5] and carriers of biological markers dyes [6].

The most important and effective synthetic strategies for the preparation of amphiphilic block copolymers involve various controlled radical polymerization methods such as Reversible Addition Fragmentation Chain Transfer (RAFT) [7], Iodine Transfer Polymerization (ITP) [8] and Atom Transfer Radical Polymerization (ATRP) [9]. The use of these efficient controlled/living radical polymerizations for the synthesis of well-defined copolymers, with different architecture resulted in a controlled molar mass of the blocks.

Atom Transfer Radical Polymerization (ATRP) is one of the most studied methods due to its robustness, versatility, monomer tolerance and mild reactions conditions [10]. This process is usually catalyzed by copper complexes, with amine ligands (L), in the  $\text{Cu}^{\text{I}}$  oxidation state. An equilibrium is established between active radicals and dormant species through a reversible redox reaction between  $\text{Cu}^{\text{I}}/\text{L}$  species and an organic halide (R-X). Important research efforts have been devoted to the reduction of the amount of metal complexes required to perform ATRP reactions. On this matter, different ATRP variations have been developed, lowering the required amount of catalyst to ppm levels to afford fast and controlled polymerizations. In our work, we focused on the supplemental activator and reducing agent SARA-ATRP [11]. The SARA-ATRP method was successfully used for controlled polymerization of a wide range of monomers like methyl methacrylate (MMA) [12], styrene (Sty) [13], and vinyl chloride (VC) [14]. This method allows preparation polymers with distinct architectures like well-defined block copolymer [15].

The literature abounds with studies using amphiphilic block copolymers of different compositions and various methods of preparation that produce nanoparticles (NPs) referred to as micelles, nanospheres, core-shell nanoparticles, micelle-like nanoparticles, crew cut micelles, nanocapsules and polymersomes [16].

A practical method developed to prepare nanoparticles is nanoprecipitation. For instance, when water is slowly added to an organic polymer solution, larger spherical particles and vesicle structures are frequently obtained. When the opposite occurs and an organic polymer solution is slowly added to water, spherical particles with small hydrodynamic radii often result [17].

Herein, we report the synthesis of a new diblock copolymer polystyrene-*b*-poly(4-vinyl dimethyl dipicolinate) PS-*b*-PVDPM by varying the ratio between blocks domain size and the preparation of nanoparticles behavior. It has been shown in previously reported works that poly(vinyldipicolinic acid) PVDPA homopolymer is an excellent chelating material for lanthanides and actinides and in particular has an excellent ability for uranium harvesting from seawater [18]. Hence, nanoparticles with PVDPA chains have a negatively chelating charged hydrophilic shell may be used for many applications i.e., luminescent nanoparticles with lanthanides-containing [19].

The self-assembly of PS-*b*-PVDPM copolymers in water performed by dialysis was studied to find the Critical Micelle Concentration (CMC) and to establish the structures formed by the copolymer above the CMC. Fluorescence spectroscopy and Dynamic Light Scattering (DLS) were used for such purpose. Fluorescence spectroscopy has been used to determine the CMC of diblock copolymer micelles. The pyrene molecule is frequently used as fluorescent probe in spectrofluorometry since its fluorescence intensity peaks at  $\lambda_{\max} = 373$  and 384 nm, denoted  $I_1$  and  $I_3$  respectively, are sensitive to the local environment [20]. Using the characteristic dependence of the fluorescence vibrational fine structure of pyrene, the so-called pyrene 1:3 ratio method has widely been used to determine the CMC [21]. By contrast, DLS is a relatively new technique for this purpose [22]. At very low concentrations, when the copolymer chains are isolated, the intensity of light scattered is weak. Above a certain concentration, when the CMC is reached in solution, the intensity of scattered light increases dramatically due to the formation of micelles.

The effect of degree of polymerization (DP) of both PS and PVDPA blocks on hydrodynamic diameter and pH-responsive behavior had been explored for the nanoparticles systems. DLS was used to study the colloidal stability of these diblock copolymer nanoparticles at different pH values and temperature while their charged characters were determined by zeta potential studies. Scanning Electron Microscope SEM and Transmission Electron Microscopy (TEM) were used to determine the morphologies of copolymer nanoparticles. CMC values were determined by using DLS and pyrene 1:3 ratio method.

### **3. Materials and methods**

#### **Materials.**

Styrene (Sty, Sigma Aldrich,  $\geq 99\%$ ) was passed through silica gel to remove the inhibitor, copper (II) chloride ( $\text{CuCl}_2$ , 98%), Benzyl chloride (BnCl,  $>98\%$ ), Tris(2-pyridylmethyl)amine (TPMA, TCI,  $>98\%$ ) were used without further purification. Tetrahydrofuran (THF, pure), sulfolane (Alfa Aesar, 99% pure), were obtained from Alfa-Aesar and Copper (0) wire ( $d = 1.0 \text{ mm}$ , density  $\approx 7.02 \text{ g/m}^3$ , 99.9% Alfa-Aesar) was activated by a quick wash in HCl (1 M)/ MeOH (1/1) then dried.

#### **Methods.**

**Size-Exclusion Chromatography (SEC):** Size Exclusion Chromatography (SEC) analysis of polymers was carried out at  $35 \text{ }^\circ\text{C}$  using THF as eluent. Typically, the polymer solution was prepared at  $4 \text{ mg}\cdot\text{mL}^{-1}$  and then filtered through  $0.45 \text{ }\mu\text{m}$  PTFE filter to remove insoluble residues. The separation system includes one guard column (Malvern TGuard) and two separation columns: 1) Viscotek LC3000L ( $300 \times 8.0 \text{ mm}$ ) and 2) ViscoGEL<sup>TM</sup> GMHH r-H ( $300 \times 7.8 \text{ mm}$ ). The intensity was recorded using a refractive index (RI) detector (Walter 410) and a multi-angle light scattering (MALS) detector (Viscotek SEC-MALS 20). A refractive index increment ( $dn/dc$ ) of  $0.185 \text{ mL}\cdot\text{g}^{-1}$  was determined experimentally and used for the determination of absolute molecular weight using OmniSec<sup>TM</sup> 5.12.467 software distributed by Malvern Panalytical.

**Nuclear magnetic resonance (NMR):** All  $^1\text{H}$  NMR spectra were recorded in  $\text{CDCl}_3$  using Bruker Avance 360 MHz at 25 °C. DOSY  $^1\text{H}$  spectra were recorded in  $\text{CDCl}_3$  on a Bruker Avance 400 MHz at 25 °C.

**Dynamic Light Scattering (DLS):** DLS was performed on a Malvern Zetasizer nano ZS instrument equipped with a He-Ne laser beam at a wavelength ( $\lambda = 632 \text{ nm}$ ) and scattering angle of 173°. The critical micelle concentration (CMC) for each micelle system was determined by first examining the micelle sample at a concentration of 0.1 mg/mL and manually setting the attenuator so that the count rate ranged around 400-900 KCPS. Then, the sample was serially diluted, and each sample was measured with this fixed attenuator. The count rate was plotted as a function of concentration, with the CMC corresponding to the intersection of the upper and lower linear trend lines.

**Fluorescence measurements:** Fluorescence measurements were performed in a fluoro-Max-4 spectrofluorometer, fluorescence emission spectra of several diblock copolymer solutions containing 2  $\mu\text{M}$  of pyrene were excited at 334 nm and its emission was recorded at 374 and 384 nm, which correspond to the first and third vibrational peaks, respectively and with use of excitation slit of 5.

**Thermogravimetric Analysis (TGA):** Thermal stability of the polymers were performed under argon at a flow rate of 20  $\text{mL}\cdot\text{min}^{-1}$  and a temperature ramp of 10  $^\circ\text{C}\cdot\text{min}^{-1}$  up to 900  $^\circ\text{C}$  using a TA Instruments SDT Q600 apparatus.

## **Experimental.**

Diblock copolymers Poly(4-vinyl dimethyl dipicolinate)-block-Polystyrene (PVDPM-b-PS) have been prepared by two methods:

### **Synthesis of the hydrophobic block homopolymer PS-Cl**

The macro-initiator polystyrene (PS-Cl) was prepared by using SARA-ATRP polymerization. A solution of  $\text{CuCl}_2$  (2.3 mg), TPMA (50 mg) and 10 mL styrene was prepared (Sty/  $\text{CuCl}_2$ / TPMA = 100 / 0.02 / 0.2). Then, 6 mL of this solution was placed in a 10 mL tube with 5 cm copper wire and 30  $\mu\text{L}$  of BnCl initiator (DP = 200). The tube was closed and placed in a preheated oil bath at 60 $^\circ\text{C}$ .

The appearance of dark green color is obvious, and the mixture becomes progressively more viscous. The monomer conversion was determined by  $^1\text{H}$  NMR in  $\text{CDCl}_3$  and the molecular weight parameters were determined by SEC analysis. The reaction solution was then diluted with DCM and the polymer was precipitated in excess methanol, filtrated, and dried under vacuum.

$\bar{M}_n = 11\ 100$  g/mol,  $\bar{M}_w / \bar{M}_n = 1.07$ .  $^1\text{H}$  NMR (360 MHz,  $\text{CDCl}_3$ ):  $\delta$  (ppm) = 1.15-2.37 (m,  $\text{CH}_2$  and CH of PS,), 4.50 (m, 1H,  $\text{CHCl}$ ), 6.28 -7.27 (m, 5H, aromatic).

### **Synthesis of amphiphilic diblock copolymer PS-b-PVDPM**

The diblock copolymer PS-b-PVDPM chains were built from the PS-Cl as the macro-initiator described above substrate by SARA-ATRP polymerization. According to our previous work [18], VDPM was synthesized with the following modification, the  $\text{PdCl}_2(\text{PPh}_3)_2$  catalyst was used instead of  $\text{Pd}(\text{OAc})_2$  for the Suzuki coupling reaction in order to increase the yield and reduce the time of reaction. VDPM (82.3 mg, 0.375 mmol), TPMA (0.87 mg, 0.003 mmol),  $\text{CuCl}_2$  (0.02 mg, 0.00015 mmol), and the copper wire at 1 cm/mL were placed in a 10 mL tube equipped with magnetic bar with 0.8 mL DMSO, with prior degassing. 88.8 mg of crude PS-Cl dissolved in 0.8 mL dioxane was added. The tube was closed and placed in a preheated oil bath at 60 °C for 2 h (S / VDPM /  $\text{BnCl}$  /  $\text{CuCl}_2$  / TPMA = 400 / 10 / 1 / 0.02 / 0.4). Monomer conversion was determined using  $^1\text{H}$  NMR in  $\text{CDCl}_3$ . The afforded product was purified by diluted with DCM and precipitation in MeOH.

$^1\text{H}$  NMR (360 MHz,  $\text{CDCl}_3$ ):  $\delta$  (ppm) = 1.20-2.08 (m,  $\text{CH}_2$  and CH of PS), 3.80-4.05 (m, 6H,  $\text{COOCH}_3$ ), 6.28-7.19 (m, 5H, aromatic).

### **Synthesis of amphiphilic diblock copolymer PVDPM-b-PS**

VDPM monomer (110.6 mg), TPMA (5.8 mg),  $\text{CuCl}_2$  (0.135 mg), DMSO (0.3 mL) and  $\text{Cu}^0$  (1cm) were placed in a 10 mL tube. 5.8  $\mu\text{L}$  of the  $\text{BnCl}$  initiator was added and the tube was closed and placed in a preheated oil bath at 60 °C. After 30 minutes, NMR showed no traces of unreacted VDPM. 2.3 mL of styrene were injected with 0.5 mL sulfolane. One hour after styrene injection, a small aliquot was sampled, and a precipitation test was done. the sample precipitated in THF, meaning that the PVDPM block is still predominant, or maybe the styrene didn't even polymerize. After 2 hours, an aliquot was completely soluble

in THF, meaning that polystyrene was successfully being built on the PVDPM block. Another 0.5 mL of sulfolane was added and the reaction kinetics monitored by NMR. At each point, an aliquot was precipitated in MeOH, filtrated and dried under vacuum.

$^1\text{H}$  NMR (360 MHz,  $\text{CDCl}_3$ ):  $\delta$  (ppm) = 1.23-2.31 (m,  $\text{CH}_2$  and CH of PS), 3.83-4.04 (m, 6H,  $\text{COOCH}_3$ ), 6.26-7.22 (m, 5H, aromatic).

### **Nanoparticles preparation**

The nanoparticles were prepared by self-assembly using a solvent displacement method with a THF/ACN-water system. In a typical procedure, the copolymer (5mg) was dissolved in 1 mL of THF and 0.5 mL of ACN. The polymer-solvents were added dropwise into 10 mL of deionized basic water (pH  $\sim$  9) with stirring, and the mixture was continually stirred overnight to form micelles. The suspension was stirred under reduced pressure and dialyzed against water for 1 day to remove organic solvents.

## **4. Results and discussion**

### **4.1 Block copolymer synthesis**

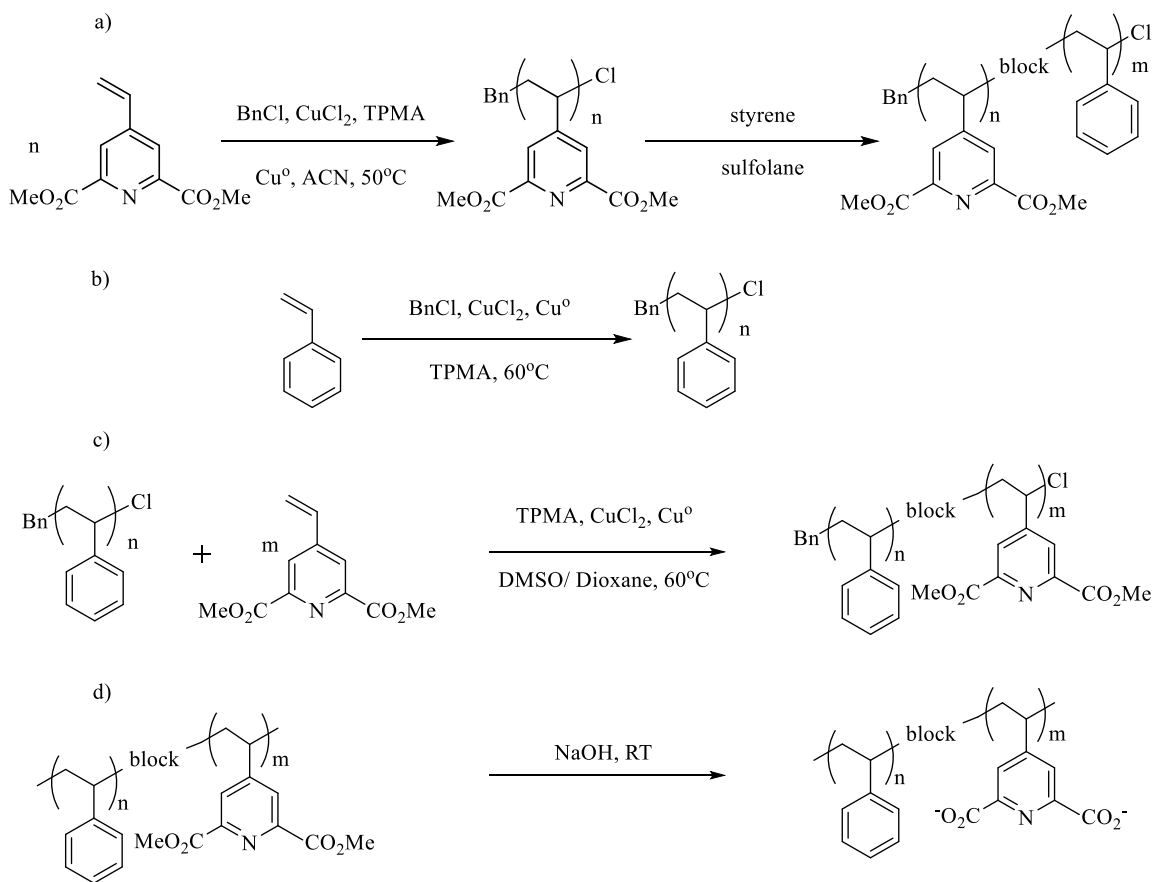
Herein, two strategies were used to synthesize the PVDPM-b-PS,. Such diblock copolymers can be derived by sequential Supplemental Activation Reducing Agent-Atom Transfer Radical Polymerization (SARA-ATRP). Scheme 1 including a) the first strategy of copolymerization (one pot reaction), b) synthesis of the polystyrene block, c) polymerization of PVDPM initiated by the PS macro-initiator and d) hydrolysis of copolymer.

The first strategy is through the polymerization of the first block of VDPM with a fixed DP = 10 using BnCl as initiator. The NMR showed a total conversion of VDPM (Equation 1 (?) a (?), see supporting information (SI)) then, the second styrene monomer can be added. Styrene conversion of PVDPM<sub>10</sub>-b-PS was monitored by NMR (Equation 2, SI). Variable polystyrene block lengths were obtained depending on reaction time (Figure SI 1, SI). Three copolymers with DP of PS equal to 184, 233 and 260 were used in this study. In this way, the DP of the first block turns out to be limited, no synthesis modification made it possible to increase the DP above 10. The second strategy consisted in the preparation of the first block of polystyrene with Cl chain end and DP = 112 leading to a



first sequence as a macro-initiator of PVDPM. Its molar mass calculated from  $^1\text{H}$  NMR and measured by SEC are very close (c.a. 11100 g/mol). The signal of the macroinitiator's Cl end group is clearly visible in NMR spectra at 4.5 ppm (Figure SI 2, SI). However, the successful copolymerization using PS-Cl as macroinitiator was observed as a broad peak of PVDPM appeared at 3.9 ppm (Figure SI 3, SI). Two copolymers with DP of PVDPM equal to 30, 50 were obtained. Thanks to these strategies, 2 blocks with control length could be afforded.

Information about PVDPM-b-PS used in this study are presented in Table 1.



Scheme 1. Synthetic routes of a) PVDPM-b-PS following two steps one pot reaction b) homopolystyrene (macro-initiator), c) amphiphilic diblock copolymer (PS-b-PVDPM) and d) hydrolysis reaction of copolymer.

#### 4.2 Diffusion data

To further demonstrate that polystyrene blocks are covalently joined with the PVDPM blocks,  $^1\text{H}$ -DOSY experiments were performed. Briefly, this method allows us to assign a

diffusion coefficient to every peak in an  $^1\text{H}$ -NMR spectrum. If two peaks are assigned to similar diffusion coefficients, it can be inferred they come from the same molecule. In  $^1\text{H}$ -DOSY plot in Figure 1a, the homopolystyrene (PS<sub>112</sub>) signal at around 2 and 6.5 ppm have a diffusion coefficient close to  $3.18 \times 10^{-10} \text{ m}^2 \text{ s}^{-1}$ . However, the signals of the diblock copolymer (PS<sub>112</sub>-b-PVDPM<sub>50</sub>) in Figure 1b, have higher diffusion coefficient of  $1.23 \times 10^{-9} \text{ m}^2 \text{ s}^{-1}$  than the signals of the PS<sub>112</sub>. Consequently, this demonstrates that the architecture of the products is indeed that of a diblock copolymer.

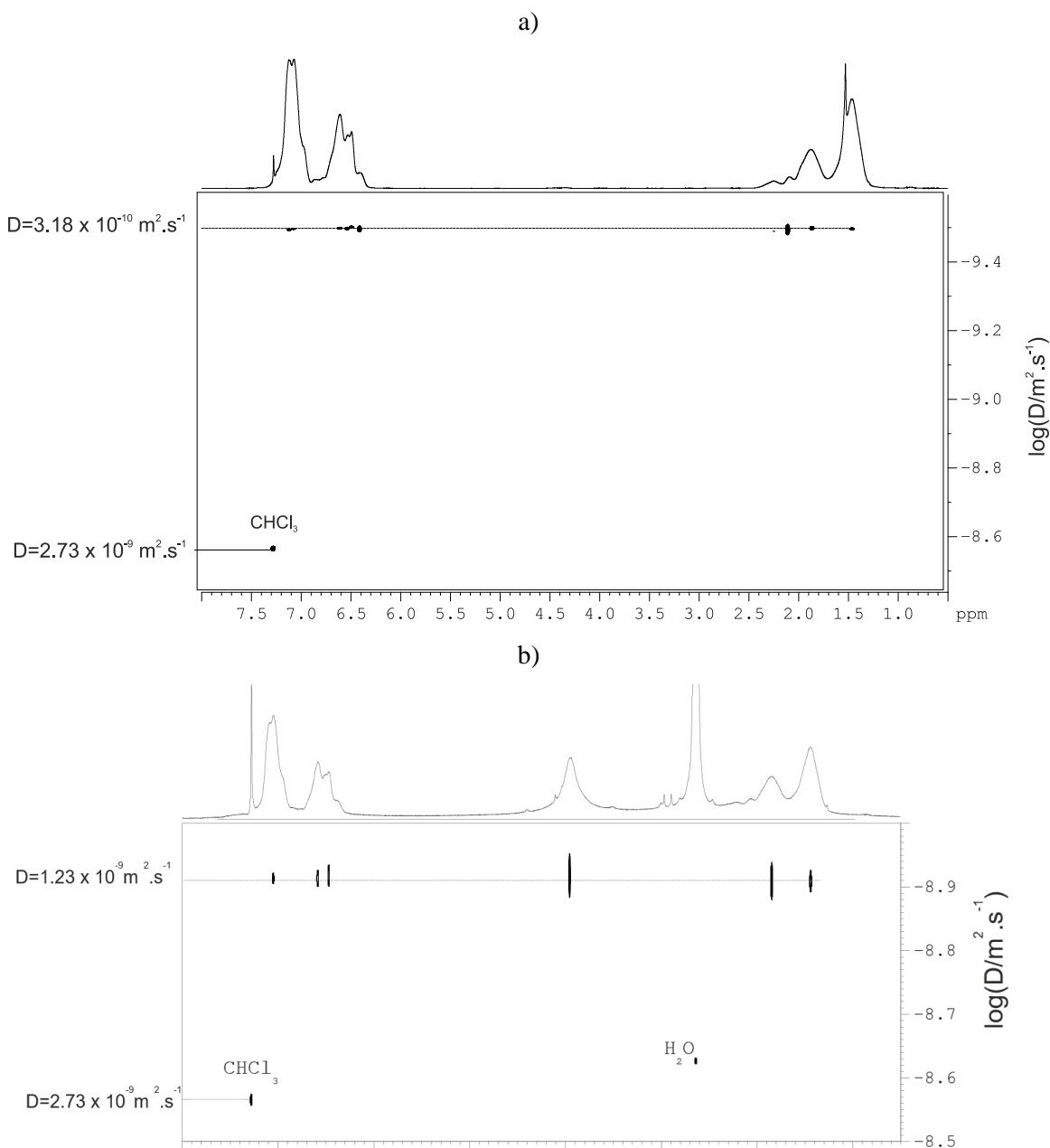


Figure 1. DOSY  $^1\text{H}$  spectrum ( $\text{CDCl}_3$ , 400 MHz, 298 K) of the sample of a) the homopolystyrene ( $\text{PS}_{112}$ ) b) the target polymerized diblock copolymer ( $\text{PS}_{112}\text{-b-PVDPM}_{50}$ )

Diblock copolymer	Time (hours)	NMR conversion (%)	$\text{MM}_{\text{NMR}}$ (g/mol)
$\text{PVDPM}_{10}\text{-b-PS}_{184}$	18	46 <sup>a</sup>	21 500
$\text{PVDPM}_{10}\text{-b-PS}_{233}$	22	58 <sup>a</sup>	26 600
$\text{PVDPM}_{10}\text{-b-PS}_{260}$	29	65 <sup>a</sup>	29 400
$\text{PS}_{112}\text{-b-PVDPM}_{30}$	3	30 <sup>b</sup>	18 400
$\text{PS}_{112}\text{-b-PVDPM}_{50}$	5	50 <sup>b</sup>	22 900

Table 1. Time of reaction, a) % of conversion of styrene (targeted DP = 400), b) % of conversion of VDPM (targeted DP = 100) and molar masses obtained by NMR.

### 4.3 Thermal characterization of polymers

Thermal stabilities of polymer ( $\text{PVDPM}_{10}$ ), copolymer ( $\text{PS}_{112}\text{-b-PVDPM}_{30}$  and  $\text{PS}_{112}\text{-b-PVDPM}_{50}$ ) and polystyrene ( $\text{PS}_{112}$ ) were established by TGA under argon atmosphere as shown in Figure 2.  $\text{PVDPM}$  and  $\text{PS}_{112}$  have only one step degradation, however,  $\text{PS}_{112}\text{-b-PVDPM}_{30}$  and  $\text{PS}_{112}\text{-b-PVDPM}_{50}$  undergo a two-step degradation. Early decrease in weight % below 100 °C is due to the loss of residual solvents. In fact, as observed in the insert figure, the  $\text{PVDPM}_{10}$  (~ 323 °C) homopolymer has much lower thermal stability than  $\text{PS}_{112}$  polystyrene (~ 410 °C).  $\text{PS}_{112}\text{-b-PVDPM}_{30}$  have a two temperature of degradation ( $T_d$ ), the first  $T_{d1}$  is around 349 °C, which corresponds to the loss of the pendant group  $\text{PVDPM}_{30}$  (~ 23% of weight loss). For  $\text{PS}_{112}\text{-b-PVDPM}_{50}$  ~ 28% of weight was lost in the first time. The second temperature ( $T_{d2}$ ) occurs between 340 °C and 830 °C, and it can be attributed to the degradation of polystyrene backbone (around 65% of weight loss). In addition, the derivative thermogravimetric (DTG) data along with the decomposition temperature ( $T_d$ ) in each degradation steps are shown in (Figure SI 4 SI).

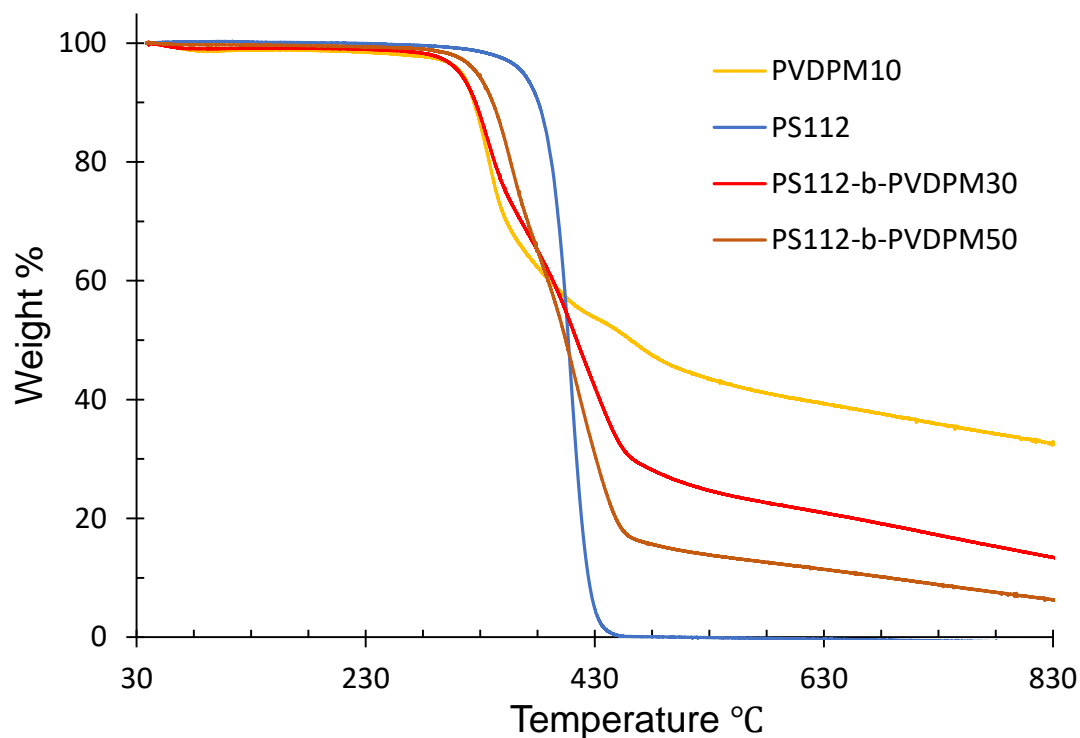


Figure 2. TGA traces of VDPM, PVDPM, PS, PVDPM<sub>30</sub>-b-PS<sub>112</sub> and PVDPM<sub>50</sub>-b-PS<sub>112</sub> with heating rate 10 °C min<sup>-1</sup> from 30 °C min<sup>-1</sup> to 830 °C min<sup>-1</sup>

#### 4.4 Nanoparticles preparation and morphology

Nanoprecipitation is based on the reduction of the quantity of the solvent in which the main composition of NPs is dissolved. At first, DLS studies of the block copolymer in organic solvent (THF/ACN) and nanoparticles in basic water were performed, suggesting particle sizes around 10 nm and 90 nm for diblock copolymer in organic solvent and nanoparticles formed in water respectively (Figure 3). Basic water (pH ~ 9) was used to transform ester to carboxylate functions as shown in Scheme 1. An explanation for the observed behavior might be the self-assembly demand of the blocks copolymer.

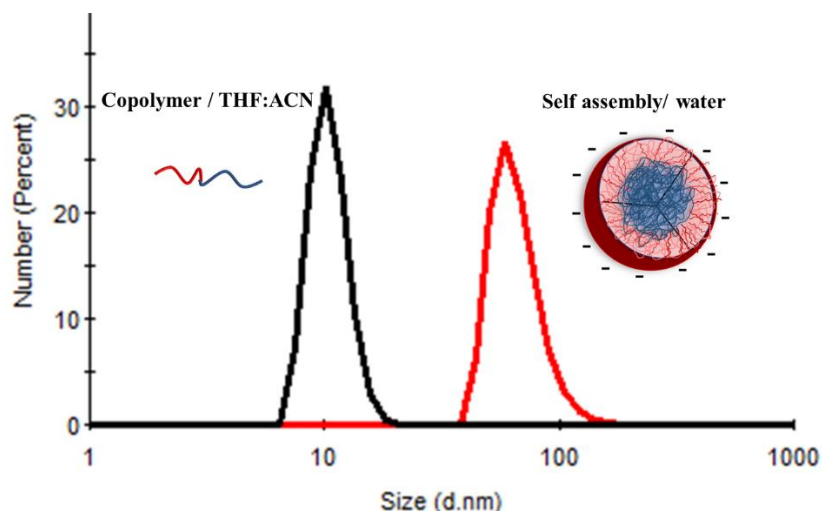


Figure 3. Hydrodynamic diameter distributions of PVDPA<sub>10</sub>-b-PS<sub>184</sub> obtained in THF/ ACN (black line) and in water (red line).

Using two different solvent displacement approaches, nanoparticles were prepared from PVDPA<sub>10</sub>-b-PS<sub>260</sub> (NP<sub>3</sub>) either by the slow addition of water (pH ~ 9) to an organic polymer solution or vice versa. As seen in Figure 4A, a broad distribution of spherical particle sizes, and the overall diameters are consistent with DLS data ( $D_h = 248$  nm, PDI = 0.1)(Figure SI 5, SI) obtained by the slow addition of water to an organic polymer solution. However, the nanoparticles prepared by the slow addition of organic polymer solution to water tend to be more uniform and smaller in size (Figure 4B) with a  $D_h$  of 120 nm and PDI of 0.01 (Figure SI 5, SI).

Based on of these observations, nanoparticles preparation, for all the synthesized copolymer, was done using the order of adding organic to water.

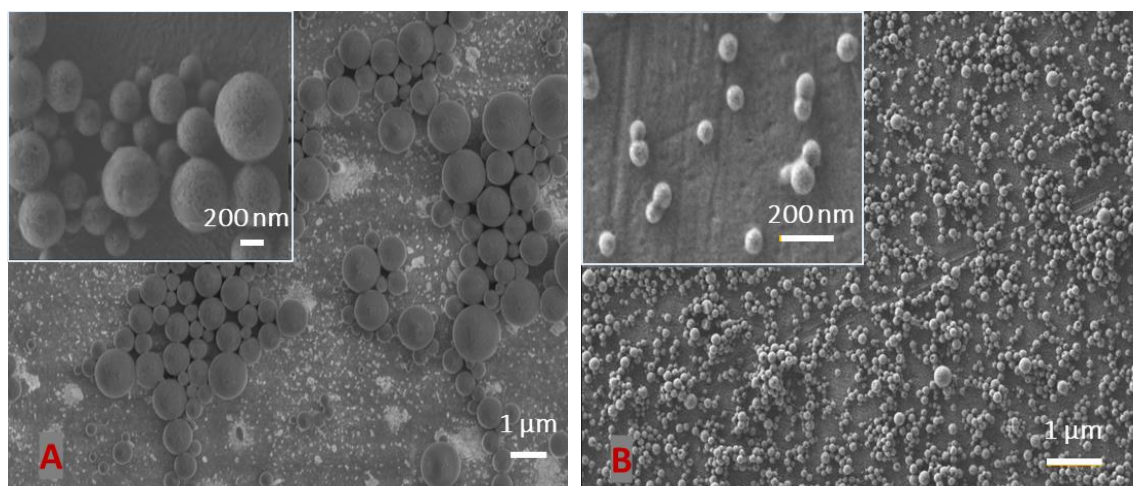


Figure 4. SEM photographs of the self-assembled nanoparticles from PVDPM<sub>10</sub>-b-PS<sub>260</sub> in aqueous solution: A) the addition of water to organic solution and B) the addition of organic solution to water.

The solution assemblies were characterized by dynamic light scattering (DLS) to determine the hydrodynamic diameter ( $D_h$ ), zeta potential ( $\zeta$ ) and polydispersity (PDI). The morphology of the nanoparticles was further investigated by SEM and TEM which allow for direct visualization of the nanostructures formed. The detailed results are shown in .

Table 2. The resulting nanoparticles had sizes between 75 and 120 nm depending on the copolymer composition.

Table 2. self-assembled nanoparticles from the PVDPA-b-PS or PS-b-PVDPA copolymers in aqueous solution at 20 °C, pH ~ 5.5.

Entry	Copolymer	$D_h$ (nm) <sup>a</sup>	$\zeta$ (mV) <sup>b</sup>	PDI <sup>c</sup>	CMC <sup>d</sup> (mg/L)	CMC <sup>e</sup> (mg/L)
NP <sub>1</sub>	PVDPA <sub>10</sub> -b-PS <sub>184</sub>	86.3 ± 2.2	-26.9	0.136	63	69
NP <sub>2</sub>	PVDPA <sub>10</sub> -b-PS <sub>233</sub>	96.3 ± 0.6	-27.2	0.044	59	56
NP <sub>3</sub>	PVDPA <sub>10</sub> -b-PS <sub>260</sub>	120.0 ± 0.4	-27.5	0.014	50	43
NP <sub>4</sub>	PS <sub>112</sub> -b-PVDPA <sub>30</sub>	75.1 ± 0.6	-37.3	0.144	40	47
NP <sub>5</sub>	PS <sub>112</sub> -b-PVDPA <sub>50</sub>	87.2 ± 1.3	-37.9	0.072	33	35

<sup>a</sup>  $D_h$  average diameter of nanoparticles <sup>b</sup>  $\zeta$  zeta potential were determined by the DLS technique. <sup>c</sup> PDI denotes the polydispersity of nanoparticles in aqueous solution. <sup>d</sup> CMC data obtained from fluorescence measurements (pyrene 1:3 ratio) and <sup>e</sup> CMC data obtained from DLS measurement.

Both the morphology and the average size of the self-assembled nanoparticles were investigated by SEM, TEM and DLS techniques. For the PVDPA-b-PS copolymers, when the weight fraction of hydrophobic (PS) block was 90 wt % within NP<sub>1</sub> sample, spherical nanoparticles were produced with an average diameter of  $86.3 \pm 2.2$  nm. However, when the weight fraction of PS increased to 92 wt % for PVDPA<sub>10</sub>-b-PS<sub>233</sub> and 96 wt% for PVDPA<sub>10</sub>-b-PS<sub>260</sub> samples, an average diameter of  $96.3 \pm 0.6$  and  $120 \pm 0.4$  was obtained, respectively. On the other hand, for the same hydrophobic head (DP = 112), when the weight fraction of PVDPA was 36 wt % within NP<sub>4</sub>, an average diameter of  $75.1 \pm 0.6$  was achieved. As for the NP<sub>5</sub> having a weight fraction of 49 wt % PVDPA the average diameter increased to  $87.2 \pm 1.3$ . All the nanoparticle suspensions had a narrow size distribution (PDI  $\leq 0.14$ ) with zeta potential ( $\geq -26.9$  mV) indicating strong electrostatic repulsions due to carboxylate anions and therefore high colloidal stability. As a note, the average size of these nanoparticles remained basically unchanged at least within 40 days at 20 °C (Figure SI 6a, SI). Moreover, these nanoparticles showed a notable stability even at high temperature (20-60°C) (Figure SI 6b, SI), suggesting a very good stability, providing them suitable for many applications.

Visualization of core-shell nanoparticles was done using TEM. Microphotographs (Figure SI 7, SI) revealed spherical particles with diameter corresponding to those obtained from DLS measurements. In TEM, the diameters of the aggregates were about 105 nm for NP<sub>3</sub>, and 60 nm for NP<sub>4</sub>. All diameters given are an average of values taken for about 20 species.

#### 4.5 CMC determination

The formation of nanoparticles of diblock copolymers was revealed using two methods. The Critical Micelle Concentration (CMC) of the block copolymer was detected by fluorescence spectroscopy using pyrene as a fluorescence probe [21]. Figure 5a shows the typical spectrum of pyrene fluorescence excited at 334 nm. The intensity of these spectra increases with increasing polymer concentration, which is one of their most notable characteristics. **Only** small changes appeared in the intensity ratio of the first and third vibrational bands, I<sub>1</sub>/I<sub>3</sub>. In the absence of nanoparticles (below CMC), pyrene senses the polar environment of methanol so the fluorescence intensity of I<sub>1</sub>/I<sub>3</sub> pyrene ratio is high. Above the CMC nanoparticles are formed, owing to the high hydrophobicity of pyrene,

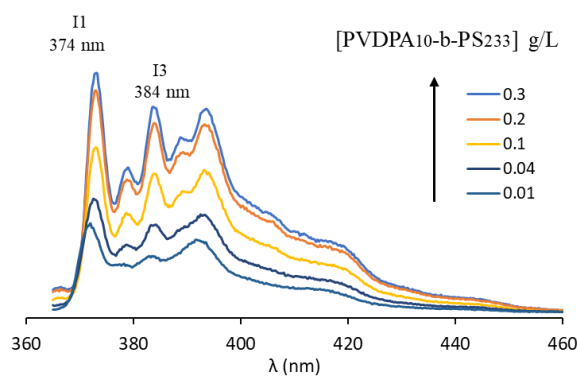
pyrene molecules are solubilized in the nanoparticles core. Because this is a non-polar solvent, the environment sensed by pyrene is less polar, and thus the  $I_1/I_3$  pyrene ratio decreases. Figure 5b shows the plot of  $I_1/I_3$  pyrene ratio versus the copolymer concentration for NP<sub>2</sub>. Those of the other nanoparticles are reported on Figure SI 8. CMC is taken as intersection of the tangent to the curve at the inflection with the horizontal tangent through the points at low polymer concentration [23]. CMC were found using the DLS method [22] with a fixed attenuator, an increase in count rate accompanied the transition from single dissolved chains to self-assembled micelles as the polymer concentration was increased. From Figure 5c, it is observed that CMC can be obtained from the intersection of the straight lines for NP<sub>2</sub>.

Table 2 obviously shows that CMCs ~~founded~~ values obtained by pyrene 1:3 ratio method are very close to those obtained by DLS method for each copolymer solution. Values for the calculated CMCs ranged from 33 to 69 g/L. The influence of the length of the hydrophilic block is negligible compared to that of the hydrophobic block [24][25]. Astafieva et al. [26] have shown that the length of the hydrophilic block on PS-b-PANa influences micellization when the hydrophobic block of the copolymer is short, i.e., about 6-110 units. So, as we can see increasing the content of hydrophilic PVDPA units in the copolymers resulted in decreasing the copolymers' CMC, as it is indicated in Table 2. The increasing number of PVDPA units in designed copolymers allowed us to investigate the effect of hydrophilic block length on their aggregation (NP<sub>4</sub> and NP<sub>5</sub>).

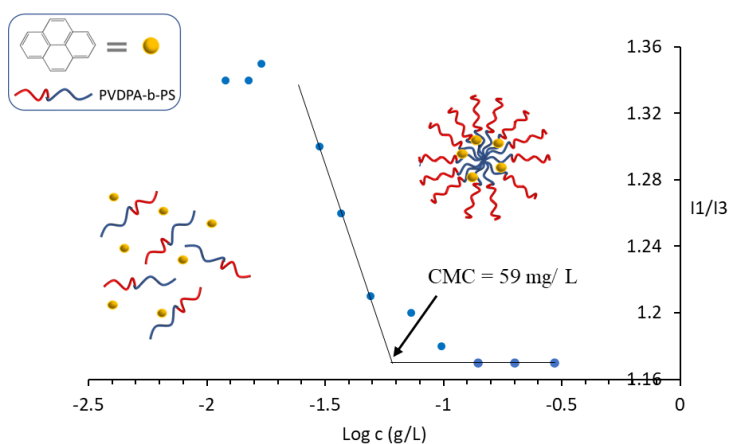
The results obtained for CMC of all the samples with fixed PVDPA equal to 10 (NP<sub>1</sub>, NP<sub>2</sub> and NP<sub>3</sub>) were displayed in Table 2 as a function of polystyrene contents. It was shown that with increasing the PS/PVDPA ratio, the CMC of the copolymers decreased. The data concluded that the CMC was decreased with the increase in polystyrene contents. This dependence is often found for amphiphilic block copolymers and was reported for several diblock copolymers [25][26].



a)



b)



c)

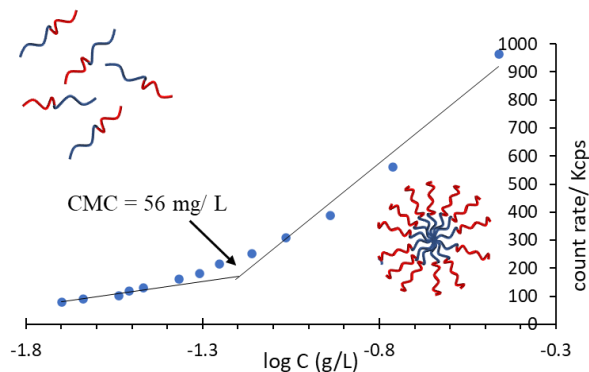
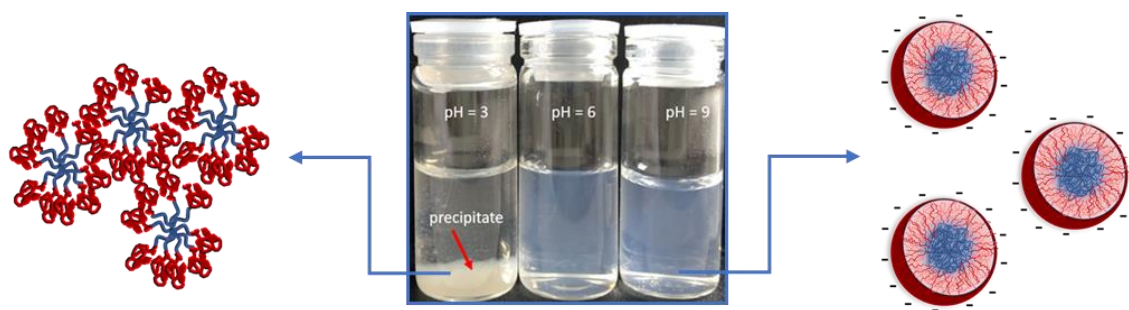


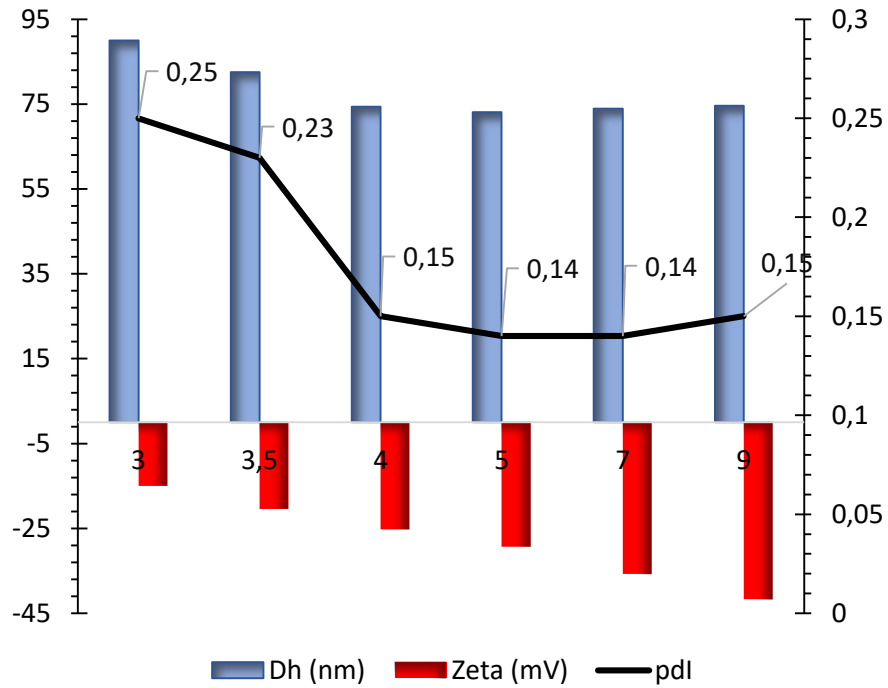
Figure 5. a) fluorescence spectra of pyrene in water in presence of increasing concentrations of diblock copolymer. The determination of the CMC for NP<sub>2</sub> using b) pyrene I<sub>1</sub>/I<sub>3</sub> ratio method and c) the count rate obtained by DLS analysis at 20°C.

#### 4.6 pH-responsive behavior of PVDPA-b-PS

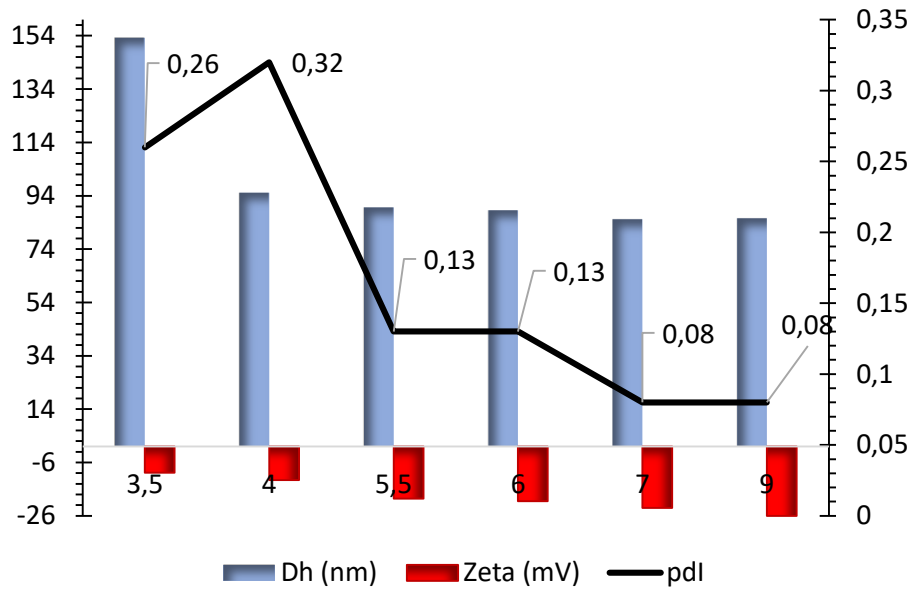
DLS was used to measure the particle sizes and zeta potential of the nanoparticles at different pH values. The original solution pH value of PVDPA-b-PS latex was 5.5 after dialysis at room temperature. Scheme 2 shows an optical observation experiment determining the colloidal stability of NP<sub>4</sub> as a function of the pH values. It revealed that precipitation occurred for this latex nanoparticle when the pH value was < 4. The white solid is, in fact, the protonated form of carboxyl PVDPA block. DLS experiments were carried out to characterize the colloidal stabilities of NP<sub>1</sub> and NP<sub>4</sub> latex with varying solution pH values Scheme 3a. The colloidal stability of NP<sub>4</sub> latex was observed above pH 4 with a  $D_h$  of  $74 \pm 1$  nm with PDI around 0.14, the particle dimension increases from 74 to 83 nm (PDI~0.23) with reducing pH values from pH 4 to pH 3.5 with appearance of a white precipitate (not detected by DLS) providing good evidence for a dispersion-to-aggregation transition. Zeta potential measurements were also correlated with the pH variation, as shown in Scheme 3a. The zeta potential of original latex was -37.3 mV indicating that colloids are highly stabilized by electrostatic repulsive force between carboxylate units of PVDPA. Once, the pH decreased, zeta potential decreased to -20.4 mV at pH 3.5. It is noteworthy to mention that, after one hour, a complete flocculation was observed. There is no doubt that the same pH-responsive behaviors of NP<sub>1</sub> and NP<sub>4</sub> latex can be attributed to the same locations of the carboxylate groups in the micellar structure. As can be seen in Scheme 3b, above pH 5.5 a slight variation on micelle diameter ( $D_h \sim 86 - 89$  nm) and on zeta potential between -20 and -26 mV was observed. However, the fast flocculation was observed when the zeta potential value decreased to -12 mV at pH 4.



Scheme 2. Macroscopic appearances of nanosuspensions at different pH.



a)



b)

Scheme 3. Variation of nanoparticles diameter (blue columns), zeta potential (red columns) and PDI (solid line) with solution pH values recorded for 0.5 g/L latex solution of a) NP<sub>4</sub> and b) NP<sub>1</sub>

## 5. Conclusion

A new class of PS-*b*-PVDPM diblock copolymer was successfully synthesized via SARA-ATRP. Nanoprecipitation was used to prepare core-shell nanoparticles in aqueous basic solution, and both the size and morphology of nanoparticles were confirmed by DLS and SEM. The core-shell nanoparticles layers exhibited the expected structure, as detected by TEM. The CMC was measured using pyrene 1:3 ratio and DLS method. The CMC decreased with increasing the length of the PS or PVDPA blocks in the copolymer chain (range 33-69 mg/L). The latex composed of PS-*b*-PVDPA is highly stable as function of time and temperature. These latexes are sensitive to the pH, the deprotonation of carboxylic acid groups of PVDPA make these latexes stable at suitable pH values ( $\text{pH} \geq 4$ ).

## 6. Acknowledgment

The authors would like to acknowledge the Lebanese National Council for Scientific Research (CNRS-L), Eiffel scholarship program of excellence and Paris-Saclay University for funding the Ph-D thesis of Abdel-wahab Mouhamad and the Lebanese National Council for Scientific Research (CNRS-L), the EU-funded project “Evaluation of the Lebanese Marine Environment (ELME)”, the French Embassy in Lebanon, and the International Atomic Energy Agency (IAEA) for granting fellowships to Dr. Nael Berri. The authors are grateful to Dr. Anne Leautic for fluorimetry experiments (ICMMO, Orsay, France).

## 7. References

1. Riess, G. Micellization of Block Copolymers. *Progress in Polymer Science (Oxford)* **2003**, *28*, 1107–1170, doi:10.1016/S0079-6700(03)00015-7
2. Nakashima, K.; Bahadur, P. Aggregation of Water-Soluble Block Copolymers in Aqueous Solutions: Recent Trends. *Advances in Colloid and Interface Science* **2006**, *123–126*, 75–96. doi:10.1016/j.cis.2006.05.016
3. Seo, D.G.; Kim, Y.M.; Ahn, H.; Moon, H.C. Non-Volatile, Phase-Transition Smart Gels Visually Indicating: In Situ Thermal Status for Sensing Applications. *Nanoscale* **2019**, *11*, 16733–16742, doi:10.1039/c9nr03686e
4. Sezgin, Z.; Yüksel, N.; Baykara, T. Preparation and Characterization of Polymeric Micelles for Solubilization of Poorly Soluble Anticancer Drugs. *European Journal of Pharmaceutics and Biopharmaceutics* **2006**, *64*, 261–268, doi:10.1016/j.ejpb.2006.06.003.
5. Kushnirov Melnitzer, V.; Sosnik, A. Hybrid Titanium Oxide/Polymer Amphiphilic Nanomaterials with Controlled Size for Drug Encapsulation and Delivery. *Advanced Functional Materials* **2020**, *30*, doi:10.1002/adfm.201806146.
6. Bronstein, L.; Krämer, E.; Berton, B.; Burger, C.; Förster, S.; Antonietti, M. Successive Use of Amphiphilic Block Copolymers as Nanoreactors and Templates: Preparation of Porous Silica with Metal Nanoparticles. *Chemistry of Materials* **1999**, *11*, 1402–1405, doi:10.1021/cm980762h.
7. Montgomery, K.S.; Davidson, R.W.M.; Cao, B.; Williams, B.; Simpson, G.W.; Nilsson, S.K.; Chiefari, J.; Fuchter, M.J. Effective Macrophage Delivery Using RAFT Copolymer Derived Nanoparticles. *Polymer Chemistry* **2018**, *9*, 131–137, doi:10.1039/c7py01363a.
8. Tonnar, J.; Lacroix-Desmazes, P.; Boutevin, B. Living Radical Ab Initio Emulsion Polymerization of N-Butyl Acrylate by Reverse Iodine Transfer Polymerization. In *Proceedings of the ACS Symposium Series* **2006**, vol. 944, pp. 605–619 (chapter 41).
9. Semsarzadeh, M.A.; Amiri, S. Silicone Macroinitiator in Atom Transfer Radical Polymerization of Styrene and Vinyl Acetate: Synthesis and Characterization of Pentablock Copolymers. *Journal of Inorganic and Organometallic Polymers and Materials* **2013**, *23*, 432–438, doi:10.1007/s10904-012-9800-y.
10. Matyjaszewski, K.; Tsarevsky, N. v. Macromolecular Engineering by Atom Transfer Radical Polymerization. *J Am Chem Soc* **2014**, *136*, 6513–6533, doi.org/10.1021/ja408069v.
11. Mendona, P. v.; Serra, A.C.; Coelho, J.F.J.; Popov, A. v.; Guliashvili, T. Ambient Temperature Rapid ATRP of Methyl Acrylate, Methyl Methacrylate and Styrene in Polar Solvents with Mixed Transition Metal Catalyst System. *European Polymer Journal* **2011**, *47*, 1460–1466, doi:10.1016/j.eurpolymj.2011.03.014.

12. Jones, G.R.; Whitfield, R.; Anastasaki, A.; Risangud, N.; Simula, A.; Keddie, D.J.; Haddleton, D.M. Cu(0)-RDRP of Methacrylates in DMSO: Importance of the Initiator. *Polymer Chemistry* **2018**, *9*, 2382–2388, doi:10.1039/c7py01196b.
13. Whitfield, R.; Anastasaki, A.; Jones, G.R.; Haddleton, D.M. Cu(0)-RDRP of Styrene: Balancing Initiator Efficiency and Dispersity. *Polymer Chemistry* **2018**, *9*, 4395–4403, doi:10.1039/c8py00814k.
14. Mendes, J.P.; Góis, J.R.; Costa, J.R.C.; Maximiano, P.; Serra, A.C.; Guliashvili, T.; Coelho, J.F.J. Ambient Temperature SARA ATRP for Meth(Acrylates), Styrene, and Vinyl Chloride Using Sulfolane/1-Butyl-3-Methylimidazolium Hexafluorophosphate-Based Mixtures. *Journal of Polymer Science, Part A: Polymer Chemistry* **2017**, *55*, 1322–1328, doi:10.1002/pola.28499.
15. Kopeć, M.; Yuan, R.; Gottlieb, E.; Abreu, C.M.R.; Song, Y.; Wang, Z.; Coelho, J.F.J.; Matyjaszewski, K.; Kowalewski, T. Polyacrylonitrile-b-Poly(Butyl Acrylate) Block Copolymers as Precursors to Mesoporous Nitrogen-Doped Carbons: Synthesis and Nanostructure. *Macromolecules* **2017**, *50*, 2759–2767, doi:10.1021/acs.macromol.6b02678.
16. Letchford, K.; Burt, H. A Review of the Formation and Classification of Amphiphilic Block Copolymer Nanoparticulate Structures: Micelles, Nanospheres, Nanocapsules and Polymersomes. *European Journal of Pharmaceutics and Biopharmaceutics* **2007**, *65*, 259–269, doi:10.1016/j.ejpb.2006.11.009.
17. Vangeyte, P.; Gautier, S.; Jérôme, R. About the Methods of Preparation of Poly(Ethylene Oxide)-b-Poly( $\epsilon$ -Caprolactone) Nanoparticles in Water - Analysis by Dynamic Light Scattering. *Colloids and Surfaces A: Physicochemical and Engineering Aspects* **2004**, *242*, 203–211, doi:10.1016/j.colsurfa.2004.04.070.
18. Maaz, M.; Elzein, T.; Barroca-Aubry, N.; Simoni, E.; Costa, L.; Nsouli, B.; Roger, P. New Insights on Uranium Recovery from Seawater and Aqueous Media. *Applied Materials Today* **2020**, *18*, doi:10.1016/j.apmt.2019.100461.
19. Thévenaz, D.C.; Monnier, C.A.; Balog, S.; Fiore, G.L. Luminescent Nanoparticles with Lanthanide-Containing Poly(Ethylene Glycol)-Poly( $\epsilon$ -Caprolactone) Block Copolymers. *Biomacromolecules* **2014**, *15*, 3994–4001, doi:10.1021/bm501058n.
20. dominguez, A.; Fernandez, A.; gonzalez, N.; Iglesias, E.; montenergro, L.J. *Determination of Critical Micelle Concentration of Some Surfactants by Three Technique*. *Journal of Chemical Education* **1997**, *75*, 1227–1232, doi:10.1021/ed074p1227.
21. Lord, D.R.C.; Duax, W.L.; Pressman, B.C.; Phillies, G.; Tokar, B.; Sanches, R. *Environmental Effects on Vibronic Band Intensities in Pyrene Monomer Fluorescence and Their Application in Studies of Micellar Systems*. *Journal of the American Chemical Society* **1977**, *99*, 2039–2044, doi:10.1021/JA00449A004.
22. Abd Karim, K.J.; Utama, R.H.; Lu, H.; Stenzel, M.H. Enhanced Drug Toxicity by Conjugation of Platinum Drugs to Polymers with Guanidine Containing Zwitterionic Functional Groups

- That Mimic Cell-Penetrating Peptides. *Polymer Chemistry* **2014**, *5*, 6600–6610, doi:10.1039/c4py00802b.
23. Aguiar, J.; Carpena, P.; Molina-Bolívar, J.A.; Carnero Ruiz, C. On the Determination of the Critical Micelle Concentration by the Pyrene 1:3 Ratio Method. *Journal of Colloid and Interface Science* **2003**, *258*, 116–122, doi:10.1016/S0021-9797(02)00082-6.
  24. Zana, R.; Marques, C.; Johner, A. Dynamics of Micelles of the Triblock Copolymers Poly(Ethylene Oxide)-Poly(Propylene Oxide)-Poly(Ethylene Oxide) in Aqueous Solution. *Advances in Colloid and Interface Science* **2006**, *123–126*, 345–351. doi:10.1016/j.cis.2006.05.011
  25. Astafieva, I.; Zhong, X.F.; Eisenberg, A. *Critical Micellization Phenomena in Block Polyelectrolyte Solutions*. *Macromolecules* **1993**, *26*, 7339-7352. doi:10.1021/MA00078A034
  26. Astafieva, I.; Khougaz, K.; Eisenberg, A. *Micellization in Block Polyelectrolyte Solutions. 2. Fluorescence Study of the Critical Micelle Concentration as a Function of Soluble Block Length and Salt Concentration*. *Macromolecules* **1995**, *28*, 7127-7134. doi:10.1021/MA00125A015
  27. Nawaz, M.; Baloch, M.K.; Price, G.J.; Ud-Din, I.; El-Mossalamy, E.S.E.B. Synthesis, Association and Surface Morphology of Poly (Ethylene Oxide)-Polystyrene Block Copolymer. *Journal of Polymer Research* **2013**, *20*, doi:10.1007/s10965-013-0180-y.
  28. Pioge, S.; Fontaine, L.; Gaillard, C.; Nicol, E.; Pascual, S. Self-Assembling Properties of Well-Defined Poly(Ethylene Oxide)-b-Poly (Ethyl Acrylate) Diblock Copolymers. *Macromolecules* **2009**, *42*, 4262–4272, doi:10.1021/ma802705b.

## Supporting information

The VDPM monomer conversion was determined using Equation

$$\text{Equation 1. VDPM conversion (\%)} = \frac{A_{3.9-4.1 \text{ ppm}} - 6}{A_{3.9-4.1 \text{ ppm}}} \times 100$$

Where  $A_{3.9-4.1 \text{ ppm}}$  represents the peak area in the region between 3.9 and 4.1 ppm and corresponds to the mixture of VDPM monomer and PVDPM. Vinyl's doublets at 5.66 and 6.17 ppm were used as 1 proton references for VDPM comonomer.

The styrene monomer conversion was determined using Equation .

$$\text{Equation 2. Styrene conversion (\%)} = \frac{A_{6.3-7.8 \text{ ppm}} - 6}{A_{6.3-7.8 \text{ ppm}} - 1} \times 100$$

Where  $A_{6.3-7.8 \text{ ppm}}$  represents the peak area in the region between 6.3 and 7.8 ppm and corresponds to the mixture of styrene monomer and polystyrene. using the vinyl doublets at 5.33 and 5.84 ppm as references for 1 proton each.

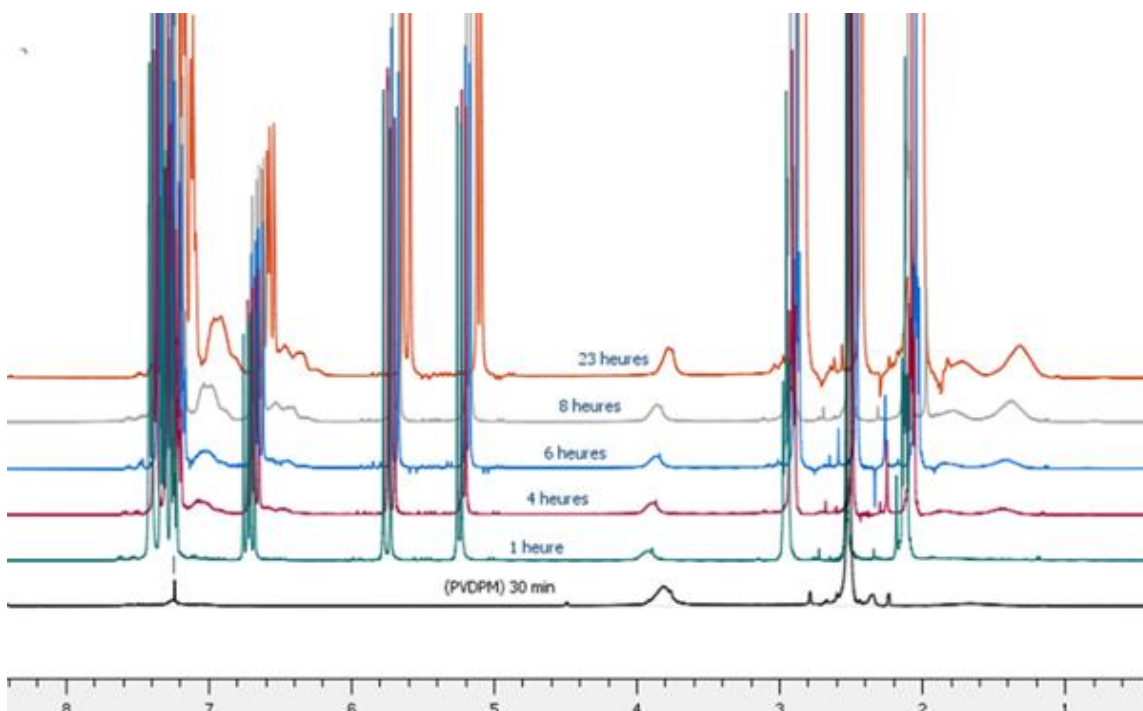


Figure SI 1. Spectra of copolymer after different reaction times



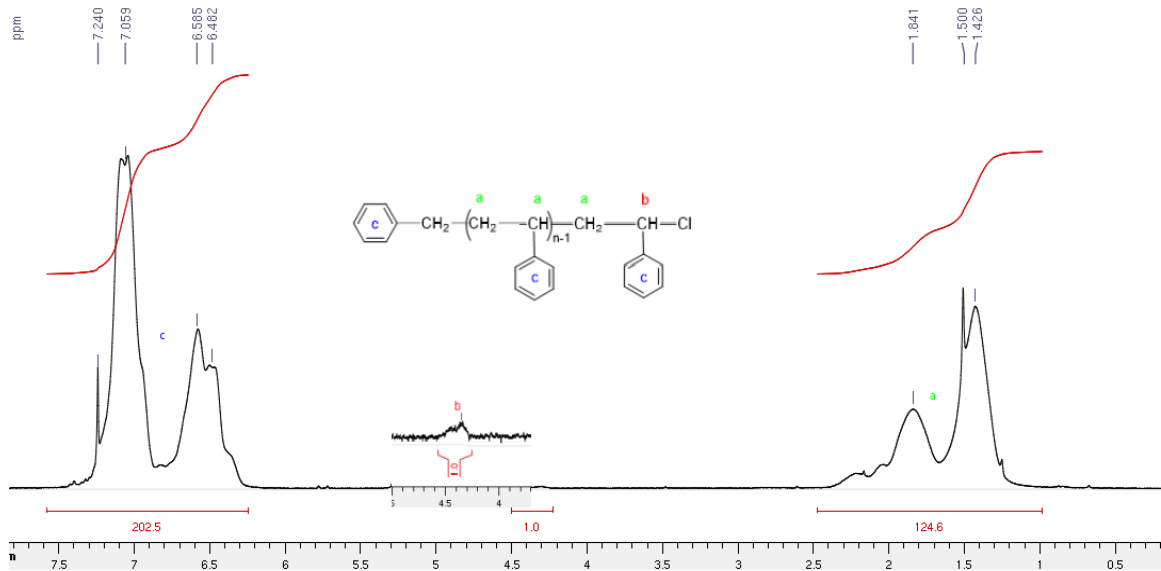


Figure SI 2.  $^1\text{H}$  NMR spectrum (360 MHz,  $\text{CDCl}_3$ ) of polystyrene PS<sub>112</sub>

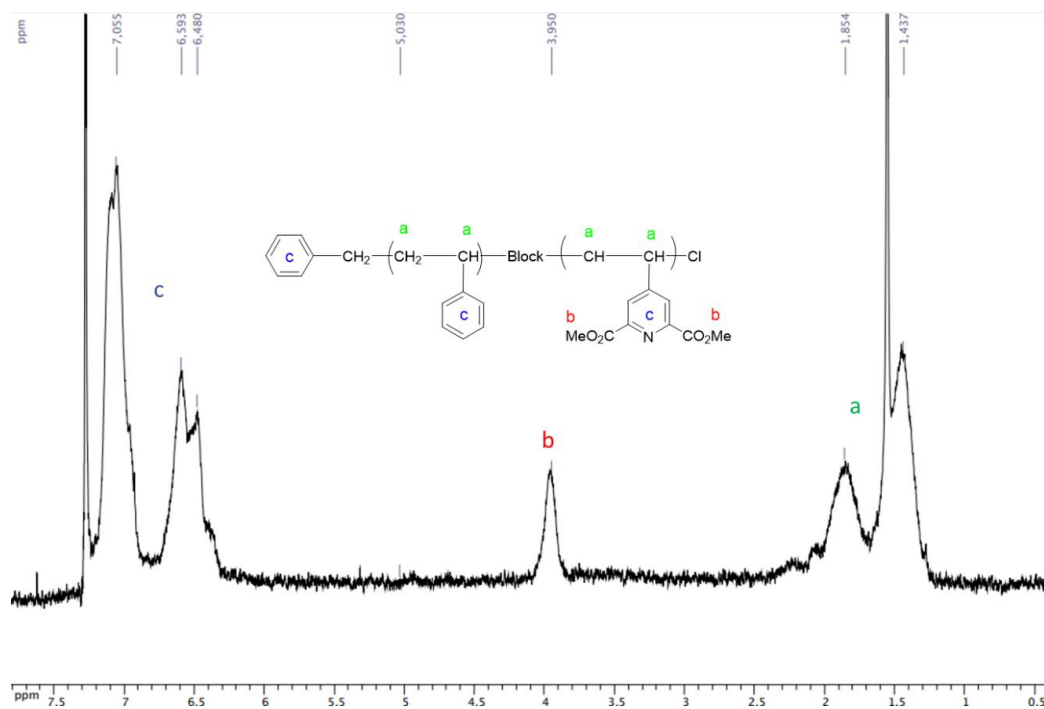


Figure SI 3.  $^1\text{H}$  NMR spectrum (360 MHz,  $\text{CDCl}_3$ ) of PS<sub>112</sub>-b-PVDPM<sub>50</sub>

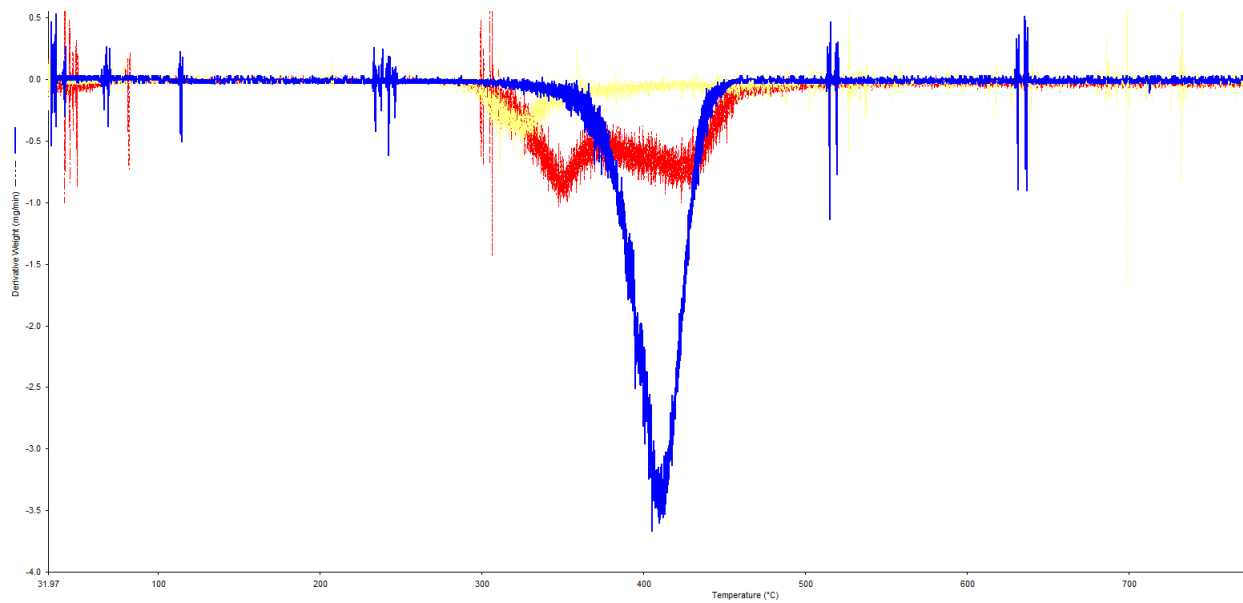


Figure SI 4. Derivative Thermogravimetric (DTG) of PVDPM10 (yellow line), PS112-b-PVDPM30 (red line), and PS112 (blue line)

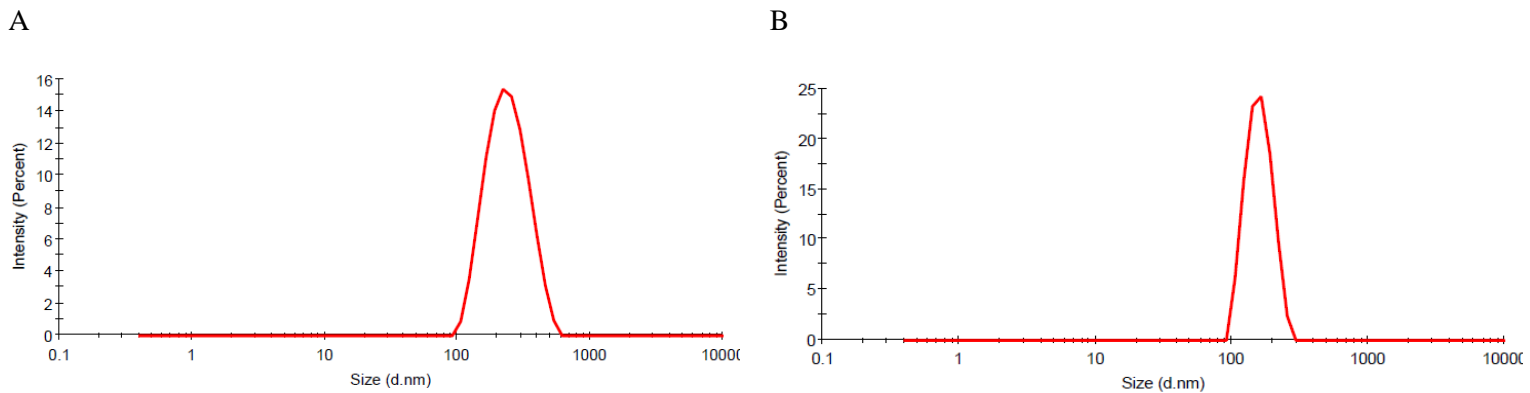
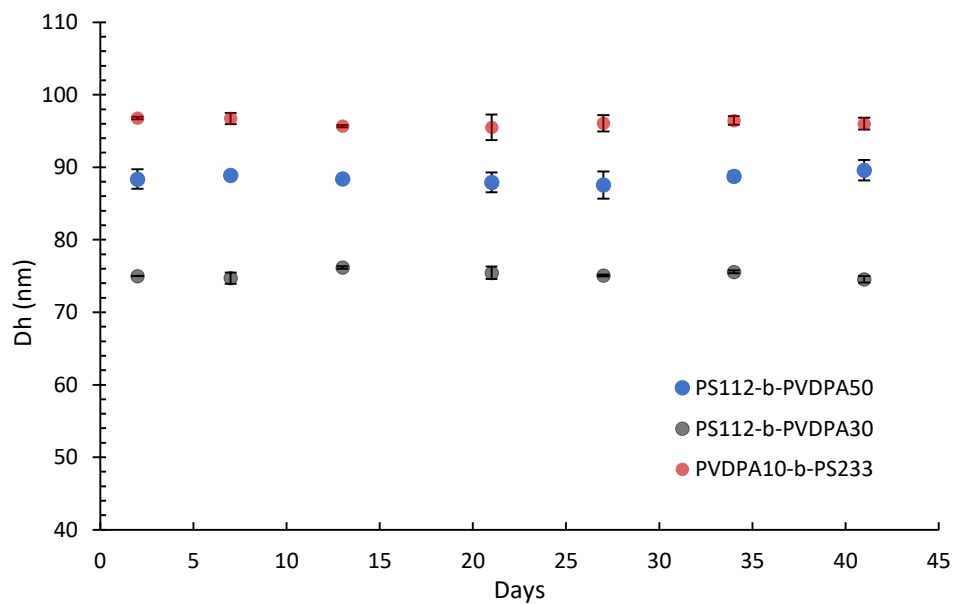


Figure SI 5. A) nanoparticles were prepared by adding water to THF/ ACN-copolymer and B) THF/ ACN-copolymer added to water using PVDPM<sub>10</sub>-b-PS<sub>260</sub>.

a)



b)

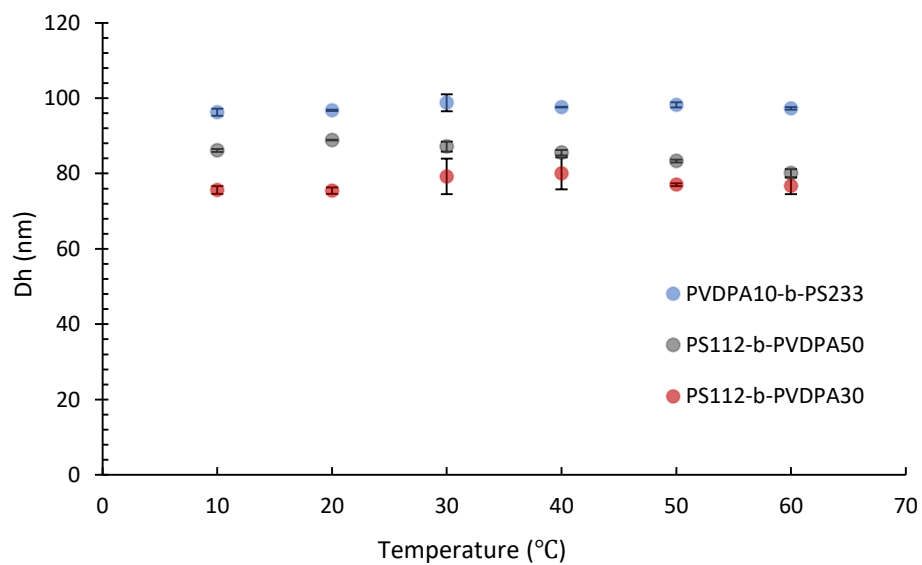
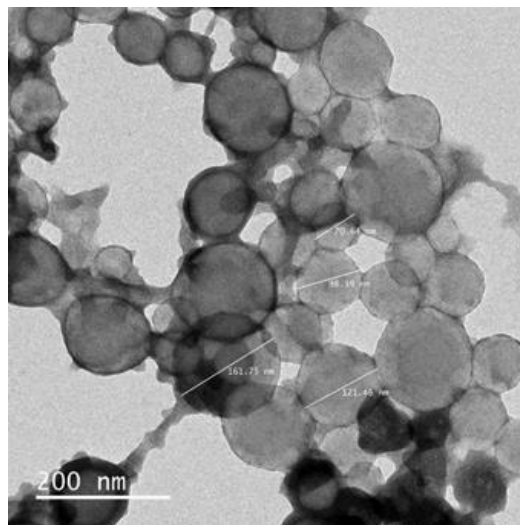


Figure SI 6. Stability of nanoparticles with a) time, b) temperature

**A**



**B**

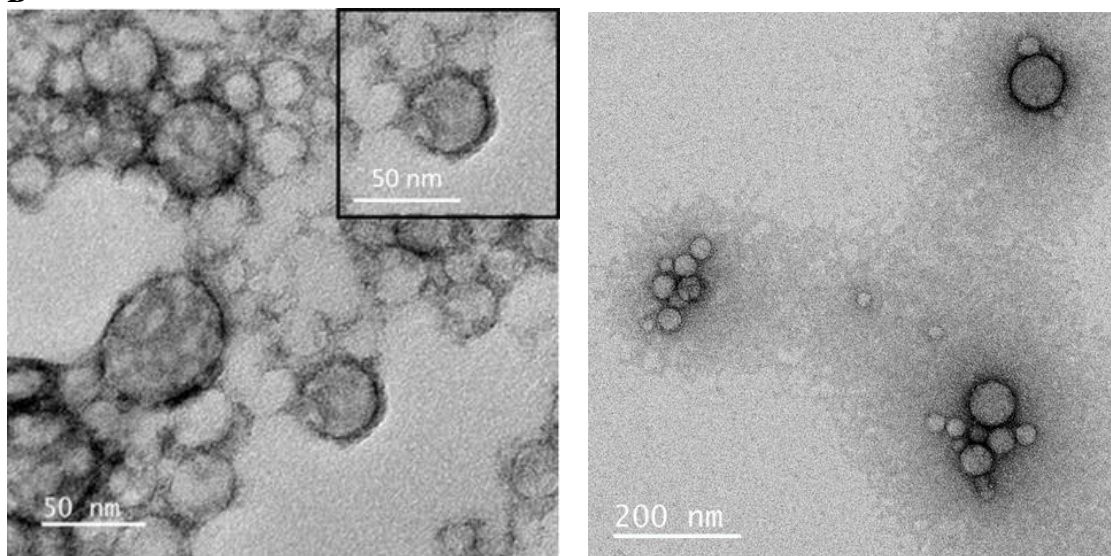


Figure SI 7. TEM images of the self-assembled nanoparticles A) NP<sub>3</sub> and B) NP<sub>4</sub> in aqueous solution.

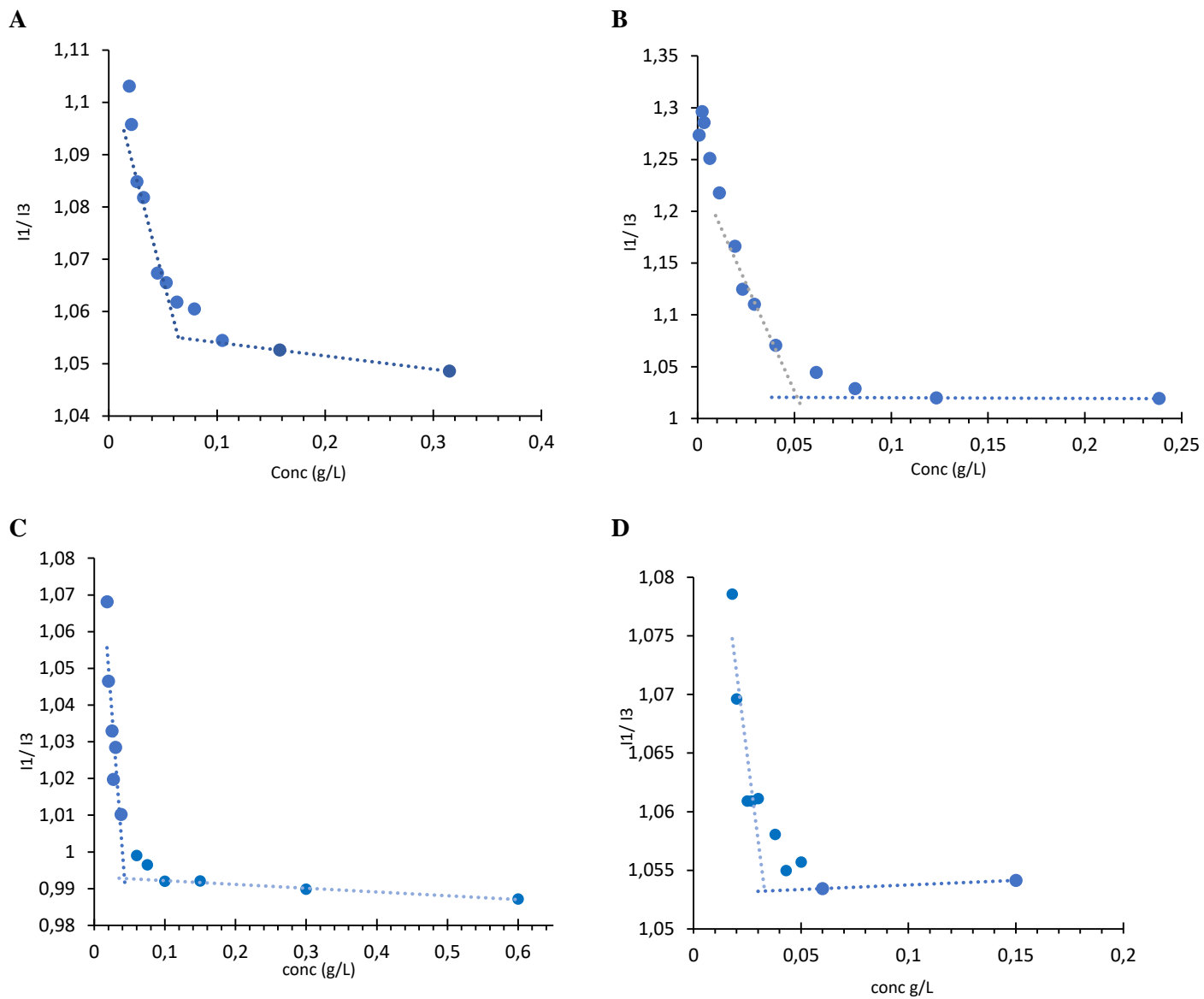


Figure SI 8. The determination of the CMC for A) NP<sub>1</sub> B) NP<sub>3</sub> C) NP<sub>4</sub> and D) NP<sub>5</sub> using ) pyrene  $I_1/I_3$  ratio method at 20°C.

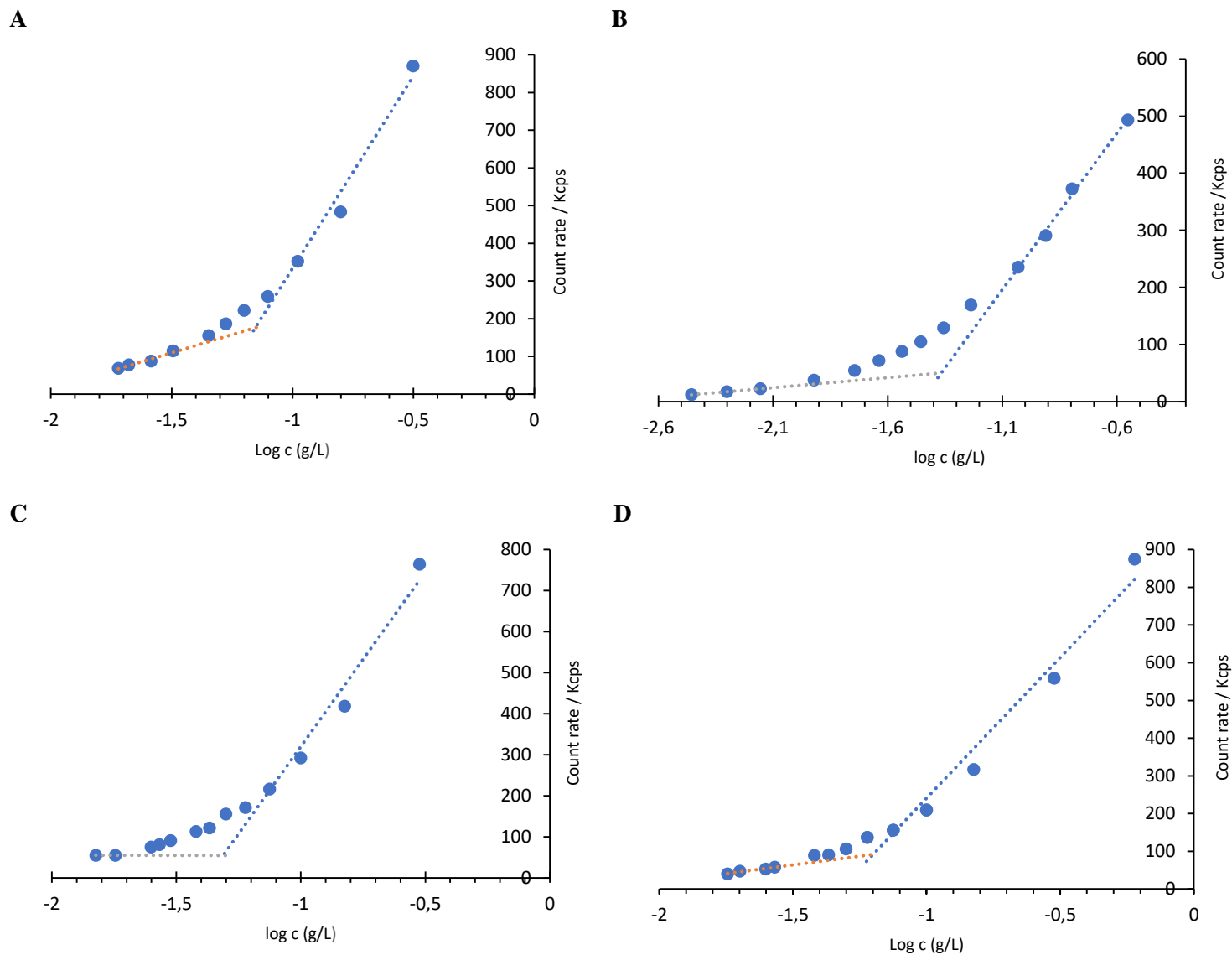


Figure SI 9. The determination of the CMC for A) NP<sub>1</sub> B) NP<sub>3</sub> C) NP<sub>4</sub> and D) NP<sub>5</sub> using the count rate method obtained by DLS analysis at 20°C.

